Journal of Food Engineering 90 (2009) 341–349

Contents lists available at ScienceDirect

Journal of Food Engineering

journal homepage: www.elsevier.com/locate/jfoodeng

Effects of drying conditions on some physical properties of soy protein films

G. Denavi [a], D.R. Tapia-Blácido [b], M.C. Añón [a], P.J.A. Sobral [c], A.N. Mauri [a,*], F.C. Menegalli [b]

[a] Centro de Investigación y Desarrollo en Criotecnología de Alimentos (CIDCA). 47 y 116, 1900 La Plata, Argentina
[b] Food Engineering Department, FEA, UNICAMP, CEP 13083-862, Campinas, SP, Brazil
[c] Food Engineering Department, FZEA-USP, P.O. Box 23, CEP 13630-000, Pirassununga, SP, Brazil

ARTICLE INFO

Article history:
Received 25 March 2008
Received in revised form 25 June 2008
Accepted 4 July 2008
Available online 10 July 2008

Keywords:
Edible films
Casting
Drying conditions
Soy proteins
Mechanical properties
Solubility

ABSTRACT

The influence of drying conditions (air temperature and relative humidity) on mechanical properties, solubility in water, and color of two kinds of soy protein isolate film: a commercial one (CSPI) and other obtained under laboratory conditions (LSPI) were evaluated using the response surface methodology (RSM). Soy protein films were prepared by casting using glycerol as plasticizer. The films were dried in a chamber with air circulation under controlled conditions of relative humidity (24%, 30%, 45%, 60%, 66%) and air temperature (34, 40, 55, 70, 76 °C). It was verified that mechanical properties of films made from LSPI and CSPI are influenced in a very different way by the drying conditions due to a diverse initial protein conformation in both materials, as was revealed by DSC and SDS–Page studies. The solubility of the LSPI film was affected by temperature and relative humidity, being lowest (~50%) for films obtained at high RH and temperatures ranging from 45 to 76 °C. For CSPI films, in contrast, solubility did not depend on the drying process and it remained relatively constant (~40%). The optimal drying conditions determined by RSM were: 70 °C and 30% RH for CSPI films and 60 °C and 60% RH for LSPI films. Dried under these conditions, CSPI films presented a higher tensile strength, lower elongation at break, lower solubility and better water and oxygen permeability than LSPI ones.

1. Introduction

The wide use of petroleum-derived plastics and the negative impact of these on the environment prompted the search for biodegradable materials obtained from renewable resources. The use of agriculture-derived biopolymers, such as proteins and polysaccharides, appears as an interesting alternative to synthetic plastics for some applications, specially those with a short life-time, such as food packaging, and generates new uses of higher added value for agriculture products (Arvanitoyannis, 1999; Ribeiro et al., 2007; Tapia-Blácido et al., 2007; Salgado et al., 2008).

In particular the use of soy proteins as film-forming agents, alone (Gennadios et al., 1996a; Cho et al., 2007) or in blend with other polymers (Cao et al., 2007; Su et al., 2007), can add value to soybean besides producing environmentally friendly biodegradable films. Soy protein produce more flexible, smooth, and clear films compared to films from other plant protein sources (Guilbert, 1986). Soy protein films are usually obtained by the casting method. This technique involves the drying of a complex colloidal solution constituted by the protein, a solvent and, usually, a plasticizer, previously poured on an appropriate support.

The effect of a specific drying condition depends on various characteristics of the raw material such as the presence of pre-existing gel phase or the occurrence of thermal gelation during drying. Besides, various phenomena may occur such as a transition from a rubbery to a vitreous phase, a phase separation (thermodynamic incompatibility) or crystallization. The interaction between the physicochemical nature of biopolymers and the drying conditions is very important.

Although a great deal of research has been done on edible films, the influence of the drying process is still neglected and poorly understood. In several works about edible films drying, variables such as relative humidity of air and the final moisture content of materials are usually not controlled, thus the influence of drying conditions is not clearly shown.

In the case of protein films, drying conditions may influence the final properties of the material as proteins can change their structure as a function of processing parameters (Tapia-Blácido et al., 2005). In this sense, temperature is a strong denaturing factor for proteins, although the thermal stability and conformation of each protein depend on the amino acid composition. During the drying period, when water is progressively eliminated, proteins conformation changes, and the degree of protein unfolding determines the type and proportion of covalent (S–S bonds) or non-covalent (hydrophobic interactions, ionic and hydrogen bonds) interactions that can be established between protein chains. It is known that

* Corresponding author. Tel./fax: +54 221 4890741.
E-mail address: anmauri@quimica.unlp.edu.ar (A.N. Mauri).

0260-8774/$ - see front matter © 2008 Elsevier Ltd. All rights reserved.
doi:10.1016/j.jfoodeng.2008.07.001

chains can interact more strongly and easily, especially by disulfide bonds, when proteins are denatured (Mauri and Añón, 2006). So the cohesion of the final network would be a function of these bonds and determines the properties of the films obtained.

Gennadios et al. (1996a) showed that it is possible to improve the moisture barrier properties of soy protein films by heat curing. Perez-Gago et al. (1999) reported that heat-denatured whey protein films had higher tensile properties than native ones. Others studies showed that heat curing improved the toughness and moisture resistance of cast protein films made with various proteins, including soy proteins (Gennadios et al., 1996b; Rhim et al., 2000). Jiang et al. (2007) reported that the mechanical properties of transglutaminase-treated soy protein isolate films vary gradually with drying temperature. Jangchud and Chinnan (1999) studied the influence of pH and drying temperature on peanut protein films, and showed that all properties improved with temperature. Working with whey proteins, Alcantara et al. (1998), verified an increase in films strength and barrier properties at higher drying rates. Nevertheless, Menegalli et al. (1999) found different results with gelatin films. Drying at high relative humidity (RH) and temperature led to gel melting and, consequently, to phase separation as well as a decrease in the drying rate.

In a previous study, the effect of the pH of the initial dispersion on the properties of soy protein films was studied (Mauri and Añón, 2006; 2008). Some differences were observed as compared to results previously published by Gennadios et al. (1993), which were attributed to differences in processing temperatures and in the initial state of the proteins.

The aim of the present study was to assess the effects of drying conditions on mechanical properties, solubility in water and color parameters of films produced from two different soybean protein isolates using an experimental design procedure. Films produced and dried on optimized conditions were also characterized regarding oxygen and water vapor barrier properties, opacity, phase properties, and microstructure.

2. Materials and methods

2.1. Materials

Two kinds of soy protein isolate were used as raw materials: a commercial one (CSPI) SUPRO 500E BATCH: E330001704, which was supplied by The Solae Company, Brazil; and an isolate obtained under laboratory conditions (LSPI). LSPI was prepared from defatted low-heat soybean meal produced by Bunge-Ceval S.A. (Brazil, PDI: 83.82 ± 0.143%). Soy flour was dispersed in distilled water (1:10 w/w). The dispersion was adjusted to pH 8.0 with 2 N NaOH, stirred at room temperature for 2 h, and centrifuged at 10,000*g* for 30 min at 15 °C. The supernatant was then adjusted to pH 4.5 with 2 N HCl and centrifuged at 3300*g* for 20 min at 4 °C. The pellet was washed with an aqueous solution at pH 4.6 and centrifuged as above. The pellet was suspended in distilled water and adjusted to pH 8.0. Finally SPI was frozen at –80 °C and freeze-dried.

The protein content of CSPI and LSPI, as measured by the Kjeldahl method, was 94 ± 2% and 91.5 ± 2% w/w, respectively, on a dry basis ($N \times 6.25$).

Glycerol (p.a. Anedra) was used as film plasticizer in all the studied conditions.

2.2. Sodium dodecyl sulfate–polyacrylamide gel electrophoresis (SDS–PAGE)

Both soy protein isolates were analyzed by SDS–PAGE according to Petruccelli and Añón (1994), using a linear gradient separating gel (4–15% in polyacrylamide) under reducing and non-reducing conditions. A continuous dissociating buffer system, containing 0.375 M Tris–HCl pH 8.8 and 0.1% w/v SDS, was used for the separating gel, while the running buffer was 0.025 M Tris–HCl, 0.192 M glycine and 0.1% w/v SDS, pH 8.3. Electrophoresis was carried out at a constant voltage of 200 V. Samples were prepared at 1% w/v in sample buffer at pH 6.8 (0.125 M Tris–HCl, 0.1% w/v SDS, 40% v/v glycerol, 0.05% w/v bromophenol blue with or without 5% w/v mercaptoethanol). Protein molecular weights were estimated using low MW markers (Pharmacia calibration kit) that included phosphorylase *b* (94,000), albumin (67,000), ovalbumin (43,000), carbonic anhydrase (30,000), trypsin inhibitor (20,100), and α-lactalbumin (14,400). Gels were fixed, stained with R-250 Coomasie blue (0.1% w/v) in water/methanol/acetic acid (5:5:2) overnight, and destained with 25% (v/v) methanol and 10% (v/v) acetic acid.

2.3. Film formation

CSPI and LSPI films were prepared by casting. Aqueous dispersions of SPI (5% w/v) and glycerol (2.5% w/v) were magnetically stirred for 20 min at room temperature. The pH was adjusted to pH 10.5 with 2 M NaOH and the dispersions were stirred for other 10 min. The films were dried in an oven with air circulation and a controlled temperature and relative humidity system (model MA 415UR, Marconi, Piracicaba, Brazil). The films were dried at 34, 40, 55, 70, 76 °C and 24%, 30%, 45%, 60%, 66% RH (Table 1) up to constant moisture content of ~25% (w.b). Previous tests on drying conditions during soy film production have shown that the final moisture content must be fixed at a value of approximately 25% (w.b) to assure that the films can be easily peeled off from the plates. To obtain films with such humidity the weight of the films was controlled (gravimetric control) during the drying step under the studied conditions, resulting in different drying times (Table 2). When the desired humidity was reached, films were removed and equilibrated for 48 h at 25 °C and 58% RH prior to the measurement of their properties. Water content of films was determined gravimetrically by drying small pieces in a ventilated oven model SE-320 (Fanem, Brazil) at 105 °C for 24 h in triplicate. The thickness of the films was measured with a digital micrometer (model FOW72-229-001, Fowler, Newcastle, CA). The mean thickness of each film was determined from an average of 20 measurements.

2.4. Mechanical properties

The tensile strength and elongation at break were determined according to the standard method D882-95 (ASTM, 1995), taking an average of five determinations in each case. The films were cut into 25.4 mm wide and 130 mm long strips using a scalpel, and mounted between the grips of the texture analyzer TA.XT2i (SMS, Surrey, England). The initial grip separation was set at 80 mm and the crosshead speed at 1.0 mm/s. The tensile strength (force/initial cross-sectional area) and elongation at break were determined directly from the stress × strain curves using the software Texture Expert V.1.15 (SMS).

2.5. Solubility in water

Solubility was measured by immersion of film disks (2.0 cm in diameter) in water containing sodium azide, at 25 ± 2 °C for a period of 24 h (Gontard et al., 1992). The amount of dry matter in the initial and final samples was determined by drying the samples at 105 °C for 24 h.

Table 1
Tensile strength (TS) and elongation at break (E) of LSPI and CSPI films obtained under different drying conditions – temperature (T) and relative humidity (RH)

Test	$T(X_1)$[a]	RH(X_2)	TS (MPa)		E (%)	
			LSPI	CSPI	LSPI	CSPI
1	40(−1)	30(−1)	0.3 ± 0.01	1.4 ± 0.01	54.5 ± 6.5	26.8 ± 2.3
2	40(−1)	60(+1)	0.3 ± 0.04	1.9 ± 0.05	96.9 ± 12.2	51.5 ± 6.1
3	70(+1)	30(−1)	0.7 ± 0.07	4.1 ± 0.01	45.1 ± 10.5	61.2 ± 2.8
4	70(+1)	60(+1)	0.9 ± 0.05	2.9 ± 0.1	69.7 ± 6.5	44.8 ± 11.6
5	33.8(−1.414)	45(0)	0.3 ± 0.03	1.9 ± 0.2	111.8 ± 10.8	38.5 ± 8.8
6	76.2(+1.414)	45(0)	1.0 ± 0.04	2.9 ± 0.2	57.9 ± 7.2	38.7 ± 9.4
7	55(0)	23.8(−1.414)	0.7 ± 0.01	2.7 ± 0.2	45.2 ± 9.8	53.3 ± 8.1
8	55(0)	66.2(+1.414)	1.2 ± 0.2	2.5 ± 0.08	97.3 ± 3.4	43.8 ± 7.0
9	55(0)	45(0)	0.8 ± 0.2	1.8 ± 0.4	81.4 ± 7.6	64.5 ± 10.3
10	55(0)	45(0)	0.8 ± 0.3	1.8 ± 0.2	85.9 ± 5.1	61.7 ± 11.0

TS: Tensile strength, E: elongation at break.
[a] Independent variables values (the values between brackets are the coded variables).

Table 2
Solubility (S), total color difference (ΔE) and drying time of LSPI and CSPI films obtained under different drying conditions – temperature (T) and relative humidity (RH)

Test	$T(X_1)$[a]	RH(X_2)	S (%)		ΔE		Time (h)	
			LSPI	CSPI	LSPI	CSPI	LSPI	CSPI
1	40(−1)	30(−1)	86.4 ± 6.0	42.8 ± 1.3	13.8 ± 1.4	17.4 ± 1.5	3.3	6.5
2	40(−1)	60(+1)	58.1 ± 1.8	39.4 ± 2.3	15.3 ± 3.2	15.7 ± 0.2	5.8	5.5
3	70(+1)	30(−1)	71.5 ± 4.7	41.1 ± 0.5	20.8 ± 3.7	14.4 ± 1.7	1.1	1.4
4	70(+1)	60(+1)	59.6 ± 3.1	37.0 ± 0.7	15.5 ± 1.2	15.1 ± 3.6	2	1.5
5	33.8(−1.414)	45(0)	95.5 ± 1.3	44.8 ± 0.9	15.7 ± 2.0	15.7 ± 1.7	11	8
6	76.2(+1.414)	45(0)	72.9 ± 1.7	38.9 ± 0.2	13.0 ± 0.4	18.5 ± 1.6	1.1	1
7	55(0)	23.8(−1.414)	80.5 ± 6.0	39.9 ± 0.9	13.4 ± 1.6	14.9 ± 0.7	1.7	5.5
8	55(0)	66.2(+1.414)	56.7 ± 2.5	40.9 ± 0.3	13.7 ± 2.2	15.3 ± 1.5	12	9
9	55(0)	45(0)	68.2 ± 0.9	41.8 ± 0.9	13.2 ± 1.5	15.9 ± 0.7	3	3
10	55(0)	45(0)	68.0 ± 0.8	39.2 ± 1.4	14.1 ± 1.0	19.3 ± 0.5	3	3.3

S: Solubility, ΔE: difference in color.
[a] Independent variables values (the values between brackets are the coded variables).

2.6. Color and opacity

Color and opacity were determined with a colorimeter (HunterLab, model Miniscan XE).

The color, represented as the difference in color (ΔE^*), was determined according to Gennadios et al. (1996b), and it was calculated as

$$\Delta E^* = \sqrt{(\Delta L^*)^2 + (\Delta a^*)^2 + (\Delta b^*)^2} \quad (1)$$

where ΔL^*, Δa^* and Δb^* are the differentials between the color parameter of the samples and of the white standard ($L^* = 94.83$, $a^* = -0.78$, $b^* = 1.44$) used as the film background.

Opacity was measured using the HunterLab method (Sobral, 1999).

2.7. Barrier properties of the films

The water vapor permeability (WVP) test was performed using a modified E96-95 ASTM Standard method (ASTM, 1995) at 25 ± 2 °C. Film samples were sealed over the circular opening of a permeation cell containing silica gel. The cells were then placed in desiccators containing distilled water. The weight loss of the cells was monitored every 24 h for 7 days.

Oxygen permeability (OP) was determined in duplicate, according to the ASTM D3985-81 (ASTM, 1995) method. The oxygen transmission rate was determined in an OX-TRAN 2/20, Mocon, Inc. (Minneapolis, MN, USA) at 25 ± 1 °C and atmospheric pressure. Oxygen permeability (OP) was calculated by dividing the oxygen transmission rate by the oxygen pressure and multiplying this result by the mean thickness of the sample.

2.8. Differential scanning calorimetry (DSC)

The thermal properties of soy protein isolates and their corresponding films were determined by differential scanning calorimetry, using a DSC TA 2010 controlled by a TA 5000 module (TA Instruments, New Castle, DE, USA), with a quench-cooling accessory. Prior to the determination, the films samples were conditioned in desiccators containing saturated solution of NaBr (58% RH), at 25 °C for three weeks. CSPI and LSPI dispersions at 20% w/w were used in these analyses. The temperature range studied was −150 to 150 °C and the heating/cooling rate was 10 °C/min.

The glass transition temperature (T_g) was considered to be the inflexion point of the base line caused by the discontinuity of the specific heat of the sample. The thermal stability of the protein was considered as the maximum peak temperature of the endothermic phenomenon.

All these properties were calculated with the Universal Analysis V1.7F software (TA Instruments) (Tapia-Blácido et al., 2007).

2.9. Scanning electron microscopy (SEM)

Small strips of film (4 mm long × 4 mm wide) were cut. These strips were fixed in a solution of 2% v/v glutaraldehyde and 0.1 M sodium cacodylate buffer (pH 7.2) for 2 h, washed with 0.1 M sodium cacodylate buffer (three times 10 min) and post-fixed in 2% w/v OsO4 (osmium tetroxide) and 0.2 M sodium cacodylate buffer (pH 7.2) for 2 h. After washing in 0.1 M sodium cacodylate buffer (three times 10 min), samples were dehydrated for 15 min through a graded ethanol series: 30%, 50%, 70% and 90% v/v, and finally for three times 15 min at 99.5% v/v, then critical point dried from

carbon dioxide. The dried samples were then mounted on aluminum stubs, coated with a thin layer of gold and observed with a JEOL Model JSM-5800LV scanning electron microscope, at an accelerated voltage of 10 kV.

2.10. Transmission electron microscopy (TEM)

Small pieces from the center of the films were prepared by fixation in 2% v/v glutaraldehyde and post-fixed in 2% w/v OsO_4. Then samples were dehydrated for 15 min in an ethanol series (30%, 50%, 70%, 90% v/v), three times for 15 min at 99.5% v/v, and two times for 20 min in propylene oxide. The samples were then embedded in increasing concentrations of propylene oxide:resin (2:1, 1:1 and 1:2) for 1 h and for 48 h in pure resin (Embed 112). The polymerization of the resin subsequently proceeded at 60 °C for 48 h. The embedded samples were sectioned in ~70 nm thick slices using a diamond knife. The sections were transferred onto supported gold grids and stained with uranyl acetate and Pb-citrate. The samples were observed with a Carl-Zeiss Model LEO906 transmission electron microscopy.

2.11. Experimental design

The effect of drying conditions (temperature and relative humidity) on the mechanical properties, color and water solubility of the films was studied with a full factorial design (2^2 plus star configuration) with two replicates at the central point. The statistical design considered and the values of the independent and coded variables are shown in Table 1.

All statistical analyses, including analysis of variance (ANOVA) and multiple comparison tests, were performed using Statistica 6.0 software. The data were fitted to a second order equation (Eq. (2)) as a function of the dependent variables.

$$Y_i = b_0 + b_1X_1 + b_2X_2 + b_{12}X_1X_2 + b_{11}X_1^2 + b_{22}X_2^2 \quad (2)$$

where b_n are constant regression coefficients, Y_i dependent variables (mechanical properties, solubility, color and drying time) and X_1 and X_2 are the coded independent variables (temperature and relative humidity).

3. Results and discussion

3.1. Soy protein isolates characterization

Both soy protein isolates were analyzed by SDS–PAGE to examine the molecular weight distribution of their polypeptides. Patterns of CSPI and LSPI not treated with mercaptoethanol are shown in Fig. 1. High molecular weight aggregates (higher than 94 kDa) are observed in CSPI, together with the polypeptide species characteristic of the β-conglycinin fraction (α of 68 kDa, α′ of 72 kDa, and β of 52 kDa polypeptides), and the acid and basic polypeptides of glycinin (A of ≅35 kDa, and B of ≅20 kDa) (Nielsen, 1985a,b). The band corresponding to the AB subunit of glycinin is not observed under non-reducing conditions, and is probably involved, together with other polypeptides, in the formation of insoluble aggregates. In the case of LSPI, the AB subunit of glycinin and acid polypetides are observed, together with low quantities of soluble aggregates of high molecular weight (higher than 94 kDa), polypeptides from the β-conglycinin fraction, and basic polypeptides from glycinin. Under reducing conditions, the characteristic patterns constituted by the α, α′, β, A and

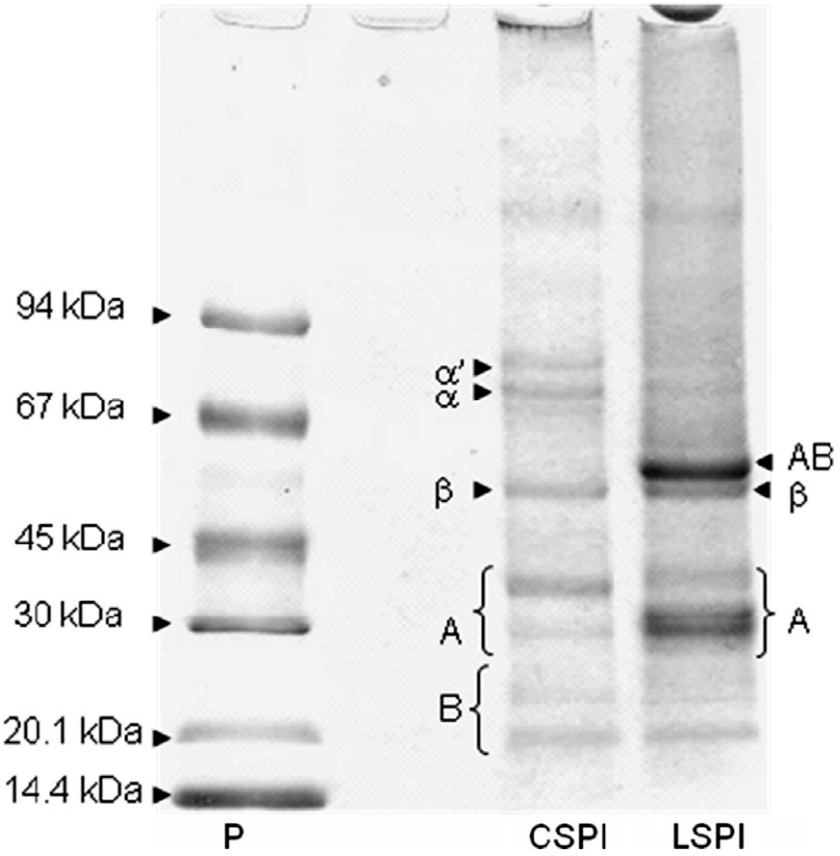

Fig. 1. SDS–PAGE patterns of the commercial soy protein isolate (CSPI), the one obtained under laboratory conditions (LSPI), and molecular weight markers (P) used to characterize soy protein polypeptides.

B subunits were observed for both isolates, CSPI and LSPI (not shown).

Fig. 2 shows the thermograms of LSPI and CSPI dispersions. LSPI dispersions showed the two typical endotherms of soybean proteins, the first at 79.03 ± 1.92 °C, corresponding to β-conglycinin denaturation, and the second at 95.06 ± 1.21 °C, corresponding to glycinin. In contrast, no endotherms were observed in the CSPI thermogram. The procedure for obtaining LSPI (without any thermal treatment of the raw material) did not affect the native conformation of soy globulins. Isolates prepared at industrial scale suffer different process in order to obtain distinctive functional properties in the final product. Thermal treatment is the most usual process used in the industry to modify proteins behavior provoking the unfolding of the macromolecules and subsequent AB β aggregation as described above (Añón et al., 2001).

3.2. Full experimental design

Tensile strength (TS) and elongation at break (E) of LSPI and CSPI films obtained according to the full experimental factorial design are shown in Table 1. Data were fitted to a second order equation (Eq. (2)) as a function of the dependent variables. Eqs. (3) and (4) represent the coded models for tensile strength (TS) and elongation at break (E) for LSPI, and Eqs. (5) and (6) represent the corresponding models for CSPI films.

$$\mathrm{TS} = 0.805 + 0.238X_1 - 0.145X_1^2 + 0.117X_2 \quad (R^2 = 0.82) \tag{3}$$

$$E = 74.58 - 14.12X_1 + 17.58X_2 \quad (R^2 = 0.81) \tag{4}$$

$$\mathrm{TS} = 1.775 + 0.632X_1 - 0.331X_1^2 + 0.428X_2^2 - 0.42X_1X_2 \quad (R^2 = 0.82) \tag{5}$$

$$E = 63.16 - 11.65X_1^2 - 6.68X_2^2 - 10.30X_1X_2 \quad (R^2 = 0.80) \tag{6}$$

Solubility (S) and total color difference (ΔE) obtained under different drying conditions regarding temperature (T) and relative humidity (RH) are shown in Table 2. Eq. (7) represents the coded model for the solubility of LSPI films.

$$S = 66.68 - 5.66X_1 + 6.60X_1^2 - 9.76X_2 \quad (R^2 = 0.83) \tag{7}$$

According to the analysis of variance (ANOVA) the coded models represented by Eqs. (4), (5), and (7) were significant at 95% of significance ($p < 0.05$) and those represented by Eqs. (3) and (6) at 90% of significance ($p < 0.1$). The solubility data for the commercial protein film (CSPI) and the color for both materials were not significantly correlated ($p > 0.05$). The responses surfaces generated using Eqs. (3)–(7) are shown in Figs. 3–5.

Tensile strength as a function of drying conditions behaved differently for each material (Fig. 3). At lower temperature, an increase of relative humidity provoked an increase of tensile strength for both materials. In contrast, these materials showed a differential response at higher temperatures: the tensile strength of LSPI films increases with relative humidity while the strength of CSPI films decreases.

At high RH, the behavior of materials is quite different: while for CSPI films the tensile strength remains virtually unchanged with the increase of temperature, those made with LSPI suffer a steep increase of tensile strength with air temperature. It is worth mentioning that absolute values of tensile strength of CSPI films are higher than those of the laboratory protein ones.

Elongations at break tendencies differed widely between materials (Fig. 4). For LSPI films, elongation increased with RH but decreased with temperature, while for CSPI films the increase of elongation with RH was marked only at low temperatures, and the decrease of elongation with temperature was significant only at high RH. For LSPI films, maximum values of elongation were

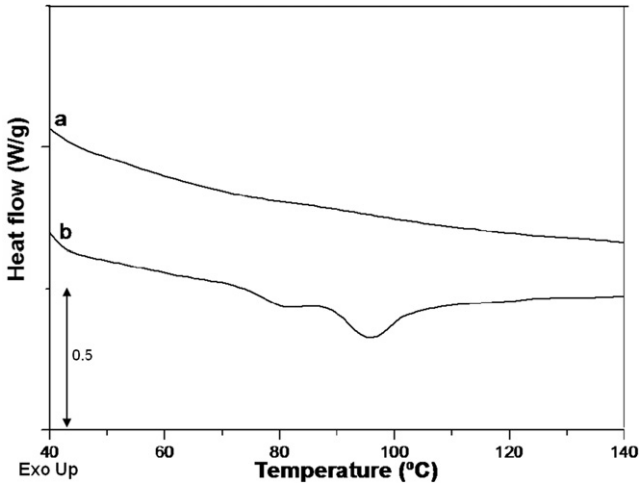

Fig. 2. DSC thermograms of (a) CSPI and (b) LSPI dispersions.

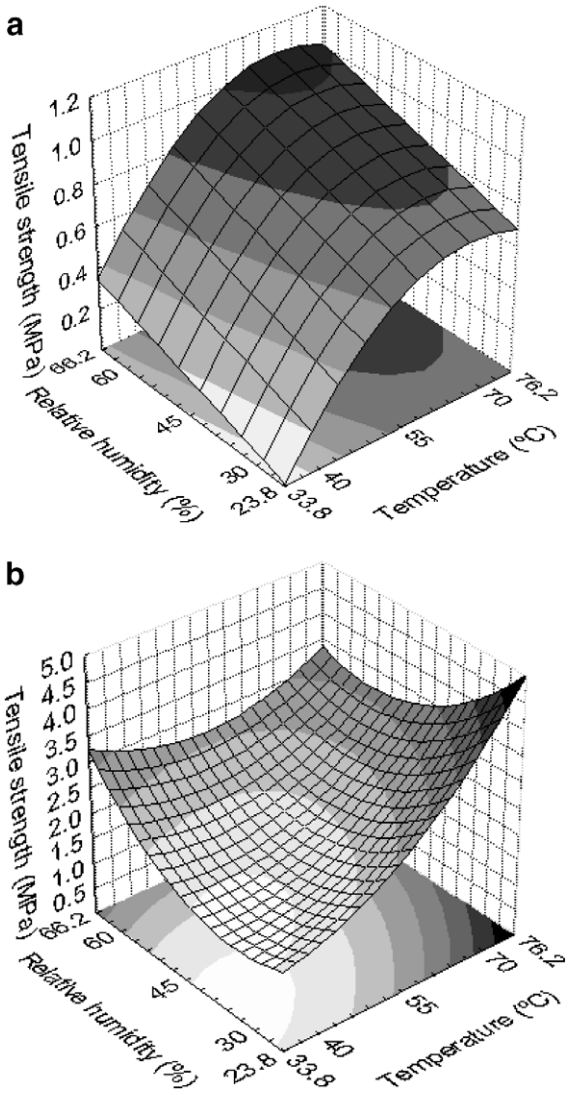

Fig. 3. Tensile strength of SPI films as a function of drying temperature and relative humidity. (a) LSPI and (b) CSPI.

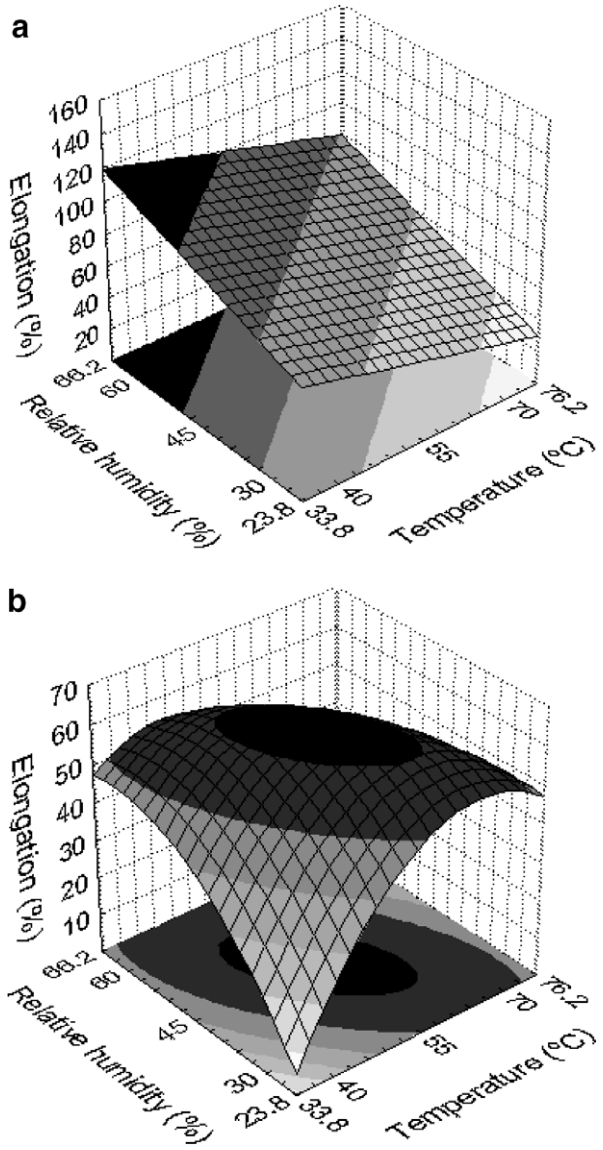

Fig. 4. Elongation at break of SPI films as a function of drying temperature and relative humidity. (a) LSPI and (b) CSPI.

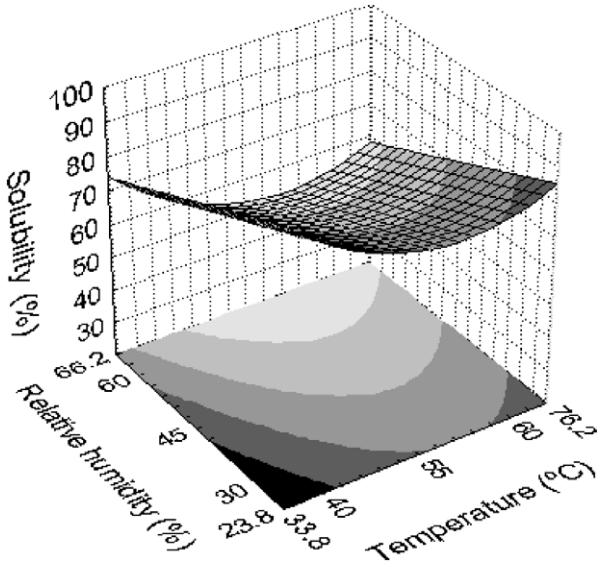

Fig. 5. Solubility of LSPI films as a function of drying temperature and relative humidity.

verified at high RH and low temperature, while for CSPI films, were measured at medium temperature (≈60 °C) at a RH range of 35–55%. Moreover, for the CSPI films *E* values ranged from 45% to 60% for nearly all conditions, while for the LSPI more extreme changes were observed (45–112%) (Table 1 and Fig. 4).

The solubility data for LSPI films was adequately correlated as a function of drying conditions (Eq. (7) and Fig. 5) but no correlation was obtained for CSPI films. For the latter, solubility does not depend of drying process and it maintains nearly constant (~40%). The minimum solubility of the LSPI films (~50%) was verified at high RH and temperatures ranging from 45 to 76 °C. In almost all conditions LSPI was more soluble than the CSPI films (Table 2). The higher solubility of LSPI films may be attributed to their higher hydrophilicity and their higher amount of solubilizing materials and their lower cross-linking (Rao et al., 2002).

Regarding the color parameters of the films (Table 2), no correlation was observed between them and the drying conditions studied, indicating that the thermal treatment of film-forming solutions during the drying step was not severe enough to produce color changes. Altered colors as a consequence of treatment have been reported in previous studies on soy protein films. Increased yellowness was reported for heated soy films, for protein reacted with the cross-linking agent dialdehyde starch, and for films obtained under alkaline conditions (Rhim et al., 2000; Kim et al., 2002; Mauri and Añón, 2008). Kim et al. (2002) explained that the lower moisture content contributed to the increased yellowness of heat-cured films. Such effect could not be observed in the present study because the final humidity of films was kept constant (~25%) under all the conditions evaluated.

3.3. Physical properties of optimized films

3.3.1. Barrier and optical properties

Films dried under optimal conditions: 60 °C and 60% RH for LSPI, and 70 °C and 30% RH for CSPI were characterized by their optical, barrier and thermal properties (Table 3). LSPI and CSPI films differed significantly in permeability to water vapor and to oxygen, according to the Tukey test ($p < 0.05$). LSPI films were more permeable to these agents than CSPI. This difference in barrier properties can be attributed to the different state of the proteins in each material as a result of the extraction procedures employed.

Although LSPI and CSPI films were not subjected to thermal treatment before drying, in contrast to film preparations extensively reported in the literature, the thermal treatment used during

Table 3
Barrier and optical properties of optimized films**

Properties	LSPI	CSPI
Moisture content (%d.b.)	25.96 ± 1.2[a]	24.46 ± 0.3[a]
WVP (g m^{-1} s^{-1} Pa^{-1})	(1.54 ± 0.12) 10^{-10a}	(1.25 ± 0.05) 10^{-10b}
Oxygen permeability (cm^3 μm m^{-2} d^{-1} kPa^{-1})	47.6 ± 9.5[a]	18.2 ± 9.5[b]
a (ao = −1.90)	−5.5 ± 0.3[a]	−3.2 ± 0.07[b]
b (bo = 2.50)	16.6 ± 1.6[a]	16.2 ± 1.1[a]
L (Lo = 95.1)	90.0 ± 1.5[a]	87.1 ± 0.9[b]
Δ*E*	15.5 ± 1.7[a]	15.9 ± 1.4[a]
Opacity	9.5 ± 3.06[a]	12.6 ± 1.02[a]
Thickness (mm)	0.076 ± 0.08[a]	0.060 ± 0.06[b]

Average ± standard deviation. Different superscript letters (a or b) denote significant difference ($p < 0.05$) between averages obtained by Tukey's test.
** Films were conditioned at 25 °C and 58% relative humidity for 48 h.

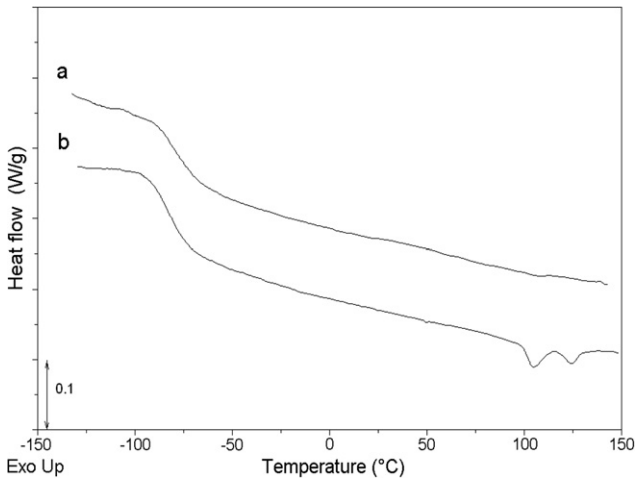

Fig. 6. DSC thermograms of SPI films obtained at the optimized drying conditions and conditioned in NaBr (58% RH) for three weeks. (a) CSPI and (b) LSPI.

drying under alkaline conditions caused the disruption of the quaternary structure of proteins accompanied by a partial protein denaturation (unfolding) (Mauri and Añón, 2006). Denaturation of soy proteins promoted the intra- and intermolecular cross-linking of amino acid residues, as well as the formation of disulfide cross-links and hydrophobic bonds (Kim et al., 2002), resulting in a better barrier to water vapor than films reported in the literature (Cho et al., 2007; Kim et al., 2002).

Table 2 also shows the values obtained for color parameters (a^*, b^* and L) and opacity of CSPI and LSPI films. No significant difference was found between CSPI and LSPI films regarding difference in color (ΔE^*) and opacity (Tukey test, $p > 0.05$). Both films were yellowish (greater value for b^*), which is typical of protein films. CSPI and LSPI films obtained in the present study were more yellowish and exhibited a higher ΔE^* (~15.50) than films prepared by Cho et al. (2007) from SPI ($\Delta E^* = 9.09 \pm 0.15$) and concentrated soy proteins ($\Delta E^* = 10.21 \pm 0.13$), which were dried at room temperature but subjected to thermal treatment (90 °C, 10 min) before drying.

3.3.2. Phase properties

Fig. 6 shows the films thermograms obtained by DSC. A glass transition (T_g) was observed at very low temperature in both thermograms (-78.8 ± 0.75 °C for CSPI and -82.36 ± 0.58 °C for LSPI). This T_g must be related with a plasticizer rich fraction and has been observed in films produced with other proteins. A glass transition eventually associated to the protein rich fraction, usually observed for various kinds of proteins, was not visible in this case (Sobral et al., 2002; Tapia-Blácido et al., 2007). Also, for LSPI film two endotherms were observed at 105.46 ± 0.2 °C and 124.46 ± 0.4 °C corresponding to the β-conglycinin and glycinin denaturation, respectively. These results agree with that presented in Fig. 2. The shift of denaturation temperatures to values higher than those depicted in Fig. 2 is due to the lower water content of films (Mauri and Añón, 2006). Consequently, although some denaturation occurs by the alkaline pH of the filmogenic solution and the drying process, some protein structure is preserved in the film of LSPI, whereas CSPI proteins are totally denatured (their thermogram did not show any endotherms).

The optimal drying conditions for CSPI were found at the highest drying rates that provoke higher shrinkage of the protein network. This is evidenced by the thinner films obtained with CSPI (60 μm) than with LPSI (75 μm), although the same methodology was used for both preparations and both films were prepared with the same dried mass per unit area.

The main difference between the two raw materials is the initial structure of their proteins which results from the method of preparation. In the case of LSPI, a process milder than the commercial one was used, which allowed to maintain the globular conformation of soybean proteins. It must be kept in mind that no thermal treatment was performed on the casting suspension before drying. Thus, as CSPI proteins presented a greater degree of unfolding during drying, their chains can interact with each other through a higher number of interactions than LSPI proteins (mainly covalent S–S links). These facts can explain why CSPI films were tougher and presented a lower solubility, and why their water and oxygen permeability were lower than those of LSPI.

When the films are prepared from the laboratory soy protein isolate, the drying process acts like a thermal treatment for the protein where the unfolding of the molecule must proceed. The best properties are obtained at higher RH and temperature, which allow a little longer time of process.

These results agree with those determined by Kim et al. (2002) working with SPI films plasticized with glycerol and dried in mild conditions. These authors demonstrated that even after the drying step, a heat treatment improved film properties. Using vacuum and temperatures ranging from 60 to 85 °C they obtained films with higher tensile strengths, and with lower elongations at break, solubilities and water permeabilities.

3.3.3. Microstructure

The microstructures of CSPI and LSPI films analyzed by SEM and TEM are presented in Figs. 7 and 8. Both films presented a dense structure, typical of protein films, as has been also reported for films prepared with amaranth proteins (Tapia-Blácido et al., 2007). The microstructure of the cross-sectional area of films revealed that LSPI film structure is dense, with a fibrous formation parallel to the film surface. Notwithstanding, some porous

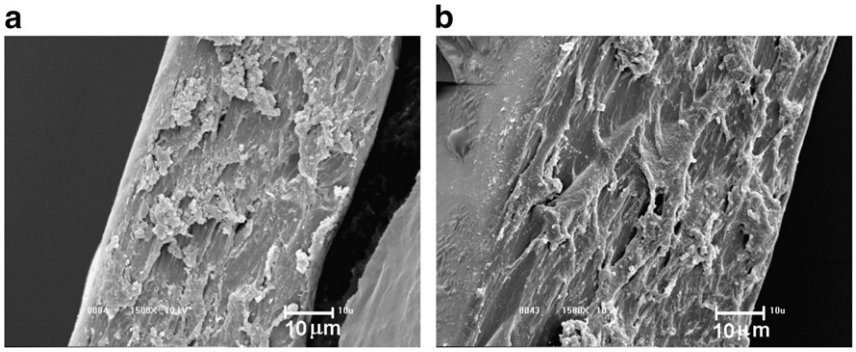

Fig. 7. SEM micrographs (×1500 magnification) of cross-sections of SPI films obtained at the optimized drying conditions of CSPI (a) and LSPI (b) films.

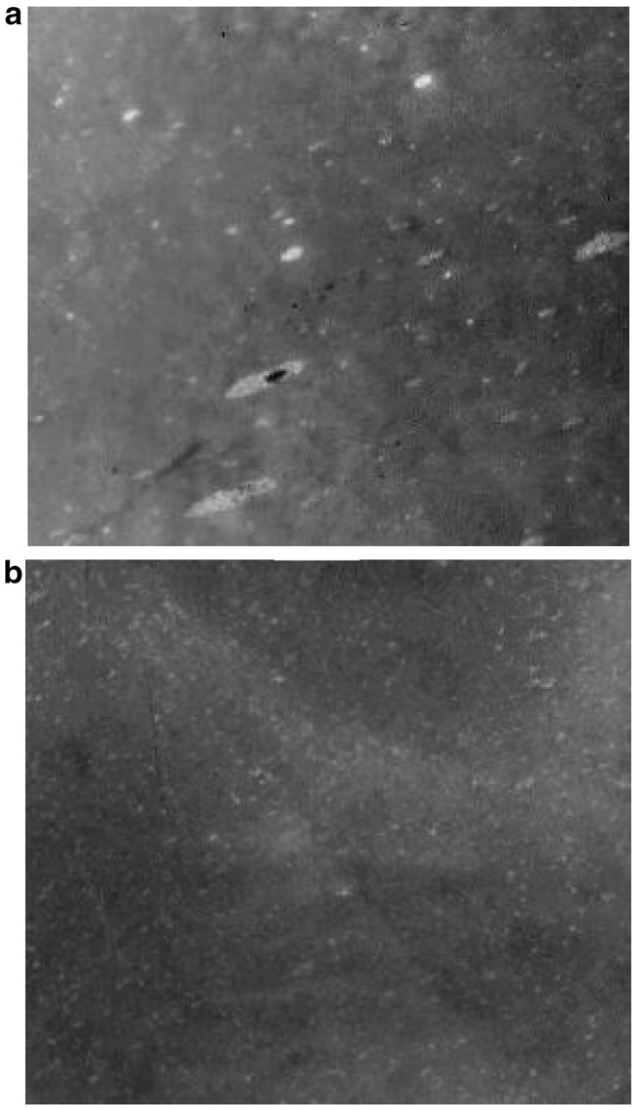

Fig. 8. TEM micrographs of SPI films obtained at the optimized drying conditions: (a) CSPI and (b) LSPI.

formation is also detected (Fig. 7), although these cavities seem to be closed porous.

As revealed by TEM, the internal microstructure of LSPI films was dense and porous, these pores probably constituting plasticization zones homogeneously distributed within the film matrix. Such pores or plasticization zones were less abundant in CSPI films. Since drying conditions were different for both films, the differences observed in film structure could be due to interactions promoted by the temperature and humidity conditions employed. CSPI films were dried at high temperature (70 °C) and low relative humidity (30%), which could have promoted the formation of a higher number of hydrophobic interactions within the film structure, while LSPI films were dried at 60 °C and high relative humidity (60%), which would promote a higher number of hydrophilic interactions. Thus, the higher number of hydrophobic interactions in the CSPI film would hamper water diffusion through the film and would confer it better barrier properties to water vapor and lower solubility than LSPI films (Tables 2 and 3). On the other hand, the presence of a higher number of pores in the structure of LSPI films (Fig. 8b) would explain the higher oxygen permeability of such films (Table 3).

4. Conclusions

This study has shown that the functional properties of soy proteins films can be modified by the temperature and relative humidity used in the drying step. It also showed that the effects of the drying conditions on the properties of soy protein films differed according to the initial structural state of the proteins. Thus, when the casting method is used, two different soy isolates with similar polypeptide composition but different unfolding of their constituent molecules (CSPI and LSPI), produce edible films with different properties even when the same drying conditions are applied for both isolates.

The analysis performed using RSM yielded the optimal drying conditions to obtain soy protein films with good mechanical properties and low solubility, these conditions being 60 °C and 60% RH for LSPI and 70 °C and 30% RH for CSPI. When obtained under these conditions, CSPI films were more resistant to break, less elongable, less soluble and less permeable to water vapor and oxygen than LSPI films. This correlated with the more dense microstructure of CSPI films compared to LSPI films, which in turn can be attributed to the greater unfolding degree of CSPI proteins which allows them to establish a higher number of interactions (mainly covalent S–S links) than in the case of LSPI proteins.

Acknowledgements

The authors wish to thank the National Agency of Scientific and Technological Support (SECyT, PICT 12085 and 35036) of Argentina, The São Paulo Research Support Foundation (FAPESP), and CyTED project XI.20, for their financial support.

References

Alcantara, C.R., Rumsey, T.R., Krochta, J.M., 1998. Drying rate effect on the properties of whey protein films. Journal of Food Process Engineering 21, 387–405.
Añón, M.C., Sorgentini, D.A., Wagner, J.R., 2001. Relationships between different hydration properties of commercial and laboratory soybean isolates. Journal of Agricultural and Food Chemistry 49, 4852–4858.
Arvanitoyannis, I.S., 1999. Totally-and-partially biodegradable polymer blends based on natural and synthetic macromolecules: preparation and physical properties and potential as food packaging materials. Journal of Macromolecular Science – Reviews in Macromolecular Chemistry and Physics C39 (2), 205–271.
ASTM, 1995. Standard test method for tensile properties of thin plastic sheeting. In: Annual book of American Standard Testing Methods. ASTM, Philadelphia, PA.
Cao, N., Fu, Y., He, J., 2007. Preparation and physical properties of soy protein isolate and gelatin composite films. Food Hydrocolloids 21 (7), 1153–1162.
Cho, S.Y., Park, J.W., Batt, H.P., Thomas, R.L., 2007. Edible films made from membrane processed soy protein concentrates. Lebensmittel-Wissenschaft und Technologie 40, 418–423.
Gennadios, A., Brandenburg, A., Weller, C., Testin, R., 1993. Effect of pH on properties of wheat gluten and soy protein isolate films. Journal of Agriculture and Food Chemistry 41, 1835–1839.
Gennadios, A., Ghorpade, V., Weller, C., Hanna, M., 1996a. Heat curing of soy protein films. Transaction of the ASAE 39, 575–579.
Gennadios, A., Weller, C., Hanna, M., Froning, M., 1996b. Mechanical and barrier properties of egg albumen films. Journal of Food Science 61, 585–589.
Gontard, N., Guilbert, S., Cuq, J., 1992. Edible wheat gluten films: influence of the main process variables on films properties using response surface methodology. Journal of Food Science 57, 190–195.
Guilbert, S., 1986. Technology and application of edible protective films. In: Mathlouthi, M. (Ed.), Food Packaging and Preservation. Elsevier Applied Science Publishers Ltd., New York, pp. 371–394.
Jangchud, A., Chinnan, M.S., 1999. Peanut protein film as affected by drying temperature and pH of film forming solution. Journal of Food Science 64, 153–157.
Jiang, Y., Tang, C.H., Wen, Q.B., Li, L., Yang, X.Q., 2007. Effect of processing parameters on the properties of transglutaminase-treated soy protein isolate films. Innovative Food Science & Emerging Technologies 8 (2), 218–225.
Kim, K., Weller, C., Hanna, M., Gennadios, A., 2002. Heat curing of soy protein films at selected temperatures and pressures. Lebensmittel-Wissenschaft und Technologie 35, 140–145.
Mauri, A.N., Añón, M.C., 2006. Effect of solution pH on solubility and some structural properties of soybean protein isolate films. Journal of the Science of Food and Agriculture 86, 1064–1072.

Mauri, A.N., Añón, M.C., 2008. Mechanical and physical properties of soy protein films with pH modified microstructures. Food Science and Technology International 14 (2), 119–125.

Menegalli, F.C., Sobral, P.J., Roques, M.A., Laurent, S., 1999. Characteristics of gelatin biofilms in relation to drying process conditions near melting. Drying Technology 17, 1697–1706.

Nielsen, N.C., 1985a. Structure of soy proteins. In: Altshul, A.M., Wilcke, H.L. (Eds.), New Proteins Foods 5: Seed Storage Proteins. Academic Press, Orlando, FL, pp. 27–60.

Nielsen, N.C., 1985b. The structure and complexity of the 11S polypeptides in soybeans. Journal of the American Oil Chemists' Society 62, 1680–1686.

Perez-Gago, M., Nadaud, P., Krochta, J., 1999. Water vapor permeability, solubility, and tensile properties of heat-denatured versus native whey protein films. Journal of Food Science 64, 1034–1037.

Petruccelli, S., Añón, M.C., 1994. Relationship between the method of obtention and the structural and functional properties of soy protein isolates. Structural and hydration properties. Journal of Agriculture and Food Chemistry 42, 2161–2169.

Rao, A., Shallo, H.E., Ericson, A.P., Thomas, R.L., 2002. Characterization of soy protein concentrate produced by membrane ultrafiltration. Journal of Food Science 67, 1412–1418.

Rhim, J., Gennadios, A., Handa, A., Weller, C., Hanna, M., 2000. Solubility, tensile, and color properties of modified soy protein isolate films. Journal of Agriculture and Food Chemistry 48, 4937–4941.

Ribeiro, C., Vicente, A., Teixeira, J., Miranda, C., 2007. Optimization of edible coating composition to retard strawberry fruit senescence. Postharvest Biology and Technology 44, 63–70.

Salgado, P., Schmidt, V., Molina Ortiz, S., Mauri, A., Laurindo, J., 2008. Biodegradable foams based on cassava starch, sunflower proteins and cellulose fibers obtained by a baking process. Journal of Food Engineering 85, 435–443.

Sobral, P., 1999. Propriedades funcionais de biofilmes de gelatina em função da espessura. Ciência & Engenharia 8, 60–67.

Sobral, P.J.A., Monterrey-Quintero, E.S., Habitante, A.M.Q.B., 2002. Glass transition of Nile tilapia myofibrillar protein films plasticized by glycerin and water. Journal of Thermal Analysis and Calorimetry 67 (2), 499–504.

Su, J.F., Huang, Z., Liu, K., Fu, L.L., Liu, H.R., 2007. Mechanical properties, biodegradation and water vapor permeability of blend films of soy protein isolate and poly (vinyl alcohol) compatibilized by glycerol. Polymer Bulletin 58 (5–6), 913–921.

Tapia-Blácido, D., Sobral, P., Menegalli, F., 2005. Effect of drying temperature and realtive humidity on the mechanical properties of amaranth flour films plasticized with glycerol. Brazilian Journal of Chemical Engineering 212, 249–256.

Tapia-Blácido, D., Mauri, A.N., Menegalli, F.C., Sobral, P.J., Añón, M.C., 2007. Contribution of starch, protein, and lipid fraction in the physical, thermal and structure properties of amaranth flour films (*Amaranthus caudatus*). Journal of Food Science 72 (5), 293–300.